

# Cloning and Expression of the Mouse Deoxyuridine Triphosphate Nucleotidohydrolase Gene: Differs From the Rat Enzyme in That it Lacks Nuclear Receptor Interacting LXXLL Motif

LIXIN KAN,<sup>1</sup> SANJAY JAIN,<sup>1</sup> WILLIAM COOK, WEN-QING CAO, NOBUTERU USUDA,  
ANJANA V. YELDANDI, M. SAMBASIVA RAO, YASHPAL S. KANWAR, AND  
JANARDAN K. REDDY<sup>2</sup>

*Department of Pathology, Northwestern University Medical School, Chicago, IL 60611*

We have previously reported the cloning of rat deoxyuridine triphosphate nucleotidohydrolase (dUTPase) cDNA and demonstrated that the full-length protein as well as the N-terminal 62-amino acid peptide interacts with peroxisome proliferator-activated receptor  $\alpha$  (PPAR $\alpha$ ). We now report the cloning of mouse dUTPase cDNA and show that it contains a 162-amino acid open reading frame, encoding a protein with a predicted  $M_r$  of 17,400 and differs from rat cDNA, which contains additional 43 amino acids at the N-terminal end. Unlike rat dUTPase, mouse dUTPase failed to bind PPAR $\alpha$ . An evaluation of 205 amino acid containing rat dUTPase cDNA revealed that the N-terminal 43 extra amino acid segment contains an LXXLL signature motif, considered necessary and sufficient for the binding of several cofactors with nuclear receptors, and its absence in murine dUTPase possibly accounts for the differential binding of these enzymes to PPAR $\alpha$ . In situ hybridization and immunohistochemical studies revealed that, in the adult mouse, dUTPase is expressed at high levels in proliferating cells of colonic mucosa, and of germinal epithelium in testis. At 9.5-day mouse embryonic development, dUTPase expression is predominantly in developing neural epithelium, and hepatic primordium, and in later developmental stages (11.5-, 13.5-, and 15.5-day embryo), the expression began to be localized to the liver, kidney, gut epithelium, thymus, granular layer of the cerebellum, and olfactory epithelium. We also show that the murine dUTPase gene comprises 6 exons and the 5'-flanking region of -1479 to -27, which exhibited high promoter activity, contains a typical TATA box and multiple *cis*-elements such as Sp-1, AP2, AP3, AP4, Ker1, RREB, and CREB binding sites. These observations suggest the existence of variants of dUTPase, some of which may influence nuclear receptor function during development and differentiation, in addition to catalyzing the hydrolysis of dUTP to dUMP.

dUTPase    PPAR    LXXLL motif    Embryonic development

---

DEOXYURIDINE triphosphate nucleotidohydrolase (dUTPase) is a ubiquitous enzyme that participates in the hydrolysis of dUTP to dUMP and inorganic pyrophosphate in prokaryotic and eukaryotic cells (31). dUTPase removes dUTP from intracellular

pools, and thus prevents it from accumulating and serving as a substrate for DNA polymerase. The inability of DNA polymerase to discriminate between dUTP and dTTP during DNA synthesis and the spontaneous deamination of cytosine present in DNA en-

---

Received October 22, 1999; accepted November 2, 1999.

<sup>1</sup>These authors contributed equally to the work.

<sup>2</sup>Address correspondence to Janardan K. Reddy, Department of Pathology, Northwestern University Medical School, 303 East Chicago Avenue, Chicago, IL 60611-3008. Tel: (312) 503-8144; Fax: (312) 503-8249; E-mail: jkreddy@nwu.edu

hance the occurrence of RNA base uracil in DNA (2). Therefore, a high concentration of dUTP leads to excessive incorporation of uracil in DNA, and under such a circumstance the excision repair pathway appears to accelerate a deleterious cycle of multiple excisions, causing mutations and/or strand fragmentation with a possibility of cell death (2,31). In this regard, it is worth noting that tumor cell death caused by chemotherapeutic agents, such as 5-fluorouracil and fluorodeoxyuridine, that inhibit thymidylate synthase and produce dramatic increases in dUTP levels, appears in part to chronic misincorporation of uracil into DNA during DNA synthesis (9). Support for this mechanism also comes from the observation that overexpression of dUTPase in human colorectal cancer cells results in resistance to fluorodeoxyuridine killing (5). Thus, a crucial role of dUTPase in maintaining DNA fidelity is well recognized.

In recent years, several laboratories have described the cloning of dUTPase cDNAs from many sources (8,12,26,28,32,35,37,42,45), and amino acid sequence comparisons revealed that these enzymes contain highly conserved motifs (8,26,34). Crystal structures of the *E. coli* (6), human (38), FIV (41), and EIAV (10) enzymes have characterized the active site and also revealed a metal ion binding site in the active site of trimeric dUTPase (10). These advances augur the development of structure-based inhibitors of dUTPase as potential cancer chemotherapeutic agents. Although our knowledge of dUTPase expression at the cellular/tissue level in mammals is somewhat limited, there is a strong suggestion that the expression of this enzyme is cell cycle and differentiation dependent (16,17,40,45). Actively dividing cells appear to possess high levels of endogenous dUTPase activity whereas terminally differentiated cells exhibit undetectable or lower levels of the enzyme, but very little is known as to how dUTPase expression is regulated during development.

We have recently found that rat dUTPase interacts with all three isoforms of peroxisome proliferator-activated receptor (PPAR $\alpha$ ,  $\delta/\beta$ , and  $\gamma$ ) and inhibits PPAR transcriptional activity in a ligand-independent manner (8). We also found that the interaction of PPAR $\alpha$  is with the N-terminal 62-amino acid segment of rat dUTPase (8). PPARs belong to the nuclear receptor superfamily of ligand-regulated transcription factors, which are closely related to the thyroid hormone receptors and retinoic acid receptors, and play well-defined roles in lipid metabolism, cellular proliferation, differentiation, and neoplastic conversion (18,33,47,52). PPAR $\alpha$  is responsible for the peroxisome proliferator-induced pleiotropic responses including liver tumorigenesis (14,29), whereas PPAR $\alpha$  plays a dominant role in adipogenic differ-

entiation (47). Although PPAR $\delta$  binds to similar target sequences as PPAR $\alpha$  and PPAR $\gamma$  isoforms, its function remains unknown. PPARs modulate the expression of specific genes by binding as heterodimers with 9-*cis*-retinoic acid (RXR) to *cis*-acting DNA sequences in target genes (23). There is considerable interest in exploring the role of coactivators and corepressors in ligand-mediated transcriptional activity of nuclear receptors in specific cell types (13,25,48,49). The identification of rat dUTPase as a PPAR-interacting protein raises interesting possibilities regarding its role in PPAR-mediated biological effects. Rat dUTPase we cloned differed from human dUTPase cDNA in that the rat enzyme was longer at the N-terminal end, although both rat and human enzymes revealed similar sequences in their overlapping regions (26,28,35,45). We now report the cloning of mouse dUTPase cDNA and show that it is similar to human nuclear dUTPase and that it fails to interact with PPAR $\alpha$ . Immunohistochemical studies using polyclonal antibodies raised against rat dUTPase revealed that dUTPase localized mostly in the nucleus and is expressed predominantly in proliferating cells in rats and mice.

## MATERIALS AND METHODS

### *Cloning of the Murine dUTPase cDNA*

A  $\lambda$ ZAP newborn mouse kidney cDNA library was prepared and screened as detailed previously (21). Briefly, about  $0.5 \times 10^6$  phage recombinants were plated on each dish, and nitrocellulose filter lifts of phage plaques prepared. The filters were hybridized with a [ $\alpha$ - $^{32}$ P]dCTP random-radiolabeled full-length rat dUTPase cDNA (8). Three positive plaques were picked and purified after screening  $2 \times 10^6$  phages. The cDNA inserts of these positive phage clones were subsequently subcloned into Bluescript II (Stratagene) and sequenced on both strands, using the dideoxy chain termination method with modified T7 DNA polymerase (Sequenase, Amersham). All three clones revealed identical cDNA sequences except that one clone was 35 nucleotides shorter than the other two at the 5' end. The cDNA in the two longest clones was 796 nucleotides long, contained an open reading frame with a termination (TAG) codon, a 337-nucleotide 3'-untranslated region with a polyadenylation tail. To obtain the missing 5' end of the mouse dUTPase cDNA, we then performed rapid amplification of 5' cDNA ends (RACE) using the Marathon cDNA amplification kit (Clontech) according to the manufacturer's protocol and the products were subcloned into pGEM-T (Promega) for identification by sequence analysis. BLAST searches identi-

fied three clones in the expressed sequence tag (EST) data banks (R75545 from mouse brain representing nucleotides 1–82; AA028806 from mouse placenta, nucleotides 1–383; and AI006680 from mouse embryo, nucleotides 5–182) that partially overlapped the sequences in the cDNA clones we isolated and also corresponded to the 5' sequence of dUTPase cDNA obtained by RACE. The full-length mouse dUTPase cDNA was then obtained by reverse transcription (RT)-polymerase chain reaction (PCR) amplification of mouse liver cDNA using Marathon cDNA amplification kit (Clontech) with the NH<sub>2</sub>-terminal sense primer 5'-TCCTGCGCGGTGGGCTCGTC-3' (nucleotides 1 to 20) and the C-terminal antisense primer 5'-CTAACTGTACCCTGGGTTTTGCCA-3' (nucleotides 761–784). The PCR products were subcloned and sequenced by automated analysis (ABI, model 377). To confirm the rat dUTPase cDNA nucleotide sequence, we first resequenced the plasmid JKR5 cloned by Chu et al. (8), and then obtained a 5'-RACE product using rat liver RNA and the primer 5'-GTGAGCGTAAGCGAGCGGAGCAG-3', which we cloned and sequenced. We also designed the primer pairs (sense primer 5'-CAGCGCCATGCCGCTCTTGTG-3' and the antisense primer 5'-CGATACAGATTACAGGCAACCAT-3') based on the rat cDNA sequence published by Chu et al. (8) and generated a full-length cDNA by RT-PCR using rat liver poly(A)<sup>+</sup> RNA.

#### *In Vitro Translation and Assay for dUTPase Binding to PPAR $\alpha$*

<sup>35</sup>S-labeling of mouse PPAR $\alpha$  was achieved by *in vitro* translation using rabbit reticulocyte lysate (Promega) and [<sup>35</sup>S]methionine (Amersham Corp.). For GST pull-down assay, mouse dUTPase cDNA was cloned into *Bam*H1 and *Eco*R1 site of pGEX-5X-2 (Pharmacia). GST rat full-length dUTPase plasmid was the same as described previously (8). Mouse and rat dUTPases were expressed as GST fusion proteins in *E. coli* JM109 and bound to glutathione-sepharose beads according to manufacturer's instructions (Pharmacia). A 10- $\mu$ l aliquot of GST-dUTPase fusion protein, loaded on glutathione-sepharose beads, was incubated with 5  $\mu$ l of [<sup>35</sup>S]methionine-labeled full-length PPAR $\alpha$  protein for 2 h at 4°C in 600  $\mu$ l of NETN (20 mM Tris-HCl, pH 7.5, 100 mM KCl, 0.7 mM EDTA, 0.05% Nonidet P-40, 1 mM phenylmethylsulfonyl fluoride). After three washes in NETN, an equal volume of 1  $\times$  SDS-polyacrylamide gel electrophoresis loading buffer was added into the beads and boiled for 5 min. Samples were resolved by SDS-polyacrylamide gel electrophoresis and autoradiographed.

#### *Northern Blotting and In Situ Hybridization*

Fifty nanograms of full-length mouse dUTPase cDNA was random primed and used as a probe to hybridize mouse multiple tissue Northern blot (Clontech). For *in situ* hybridization, mouse embryos from embryonic (E) 9.5 days, E11.5 days, E13.5 days, and E15.5 days and adult mouse tissues were immersed in 4% paraformaldehyde for 16–20 h at 4°C and processed as described previously (20). Sections 5  $\mu$ m thick were cut under ribonuclease-free conditions and every sixth sagittal section for the embryos and every 10th section for the adult tissues were stained with hematoxylin and eosin for histological comparison. Mouse dUTPase cDNA, cloned in pGEM-T (Promega) was used to generate [<sup>35</sup>S]UTP-labeled sense and antisense riboprobes, and *in situ* hybridization and developing were performed as previously outlined (20). The samples were exposed typically for 10 days and Hoechst dye was used as the counterstain for histological identification. All images were visualized on the Leica DMR microscope and acquired digitally with Spot2 camera (Diagnostic Instruments).

#### *Immunohistochemistry*

Sections were deparaffinized in xylene, hydrated, and subjected to microwave antigen retrieval method in 10 mM citrate buffer, pH 6.0, for 10 min. They were then incubated for 3 h with goat anti-rat dUTPase (1:750) raised in goat (2) and the antigen-antibody complexes were visualized using Vectastain ABC immunoperoxidase reagents (Vector Labs). Proliferating cell nuclear antigen (PCNA) (3) was localized by using monoclonal antibodies (DAKO).

#### *Isolation of Mouse Genomic Clone and Localization of Intron/Exon Junctions*

Three P1 genomic clones (18864, 18865, and 18866) containing the mouse dUTPase gene were obtained by screening a mouse P1 library (mouse ES-129/Ola genomic DNA in pAd10SacII vector, Genome Systems, St. Louis, MO). These P1 clones were digested with appropriate restriction enzymes and subcloned as necessary. Clones 18864 and 18865 contained the entire dUTPase gene; we used clone 18865 for determining the intron sizes and positions by Southern blotting, restriction mapping, and sequencing.

#### *Primer Extension Analysis*

The transcription initiation site of the mouse dUTPase gene was determined using a primer 5'-CGTGC GAGAGCCTACCCGCCGAAATCTCC-3' (nucleotides 27–55; see Fig. 1) end labeled with [ $\gamma$ -<sup>32</sup>P]ATP

```

tctctcgcagcgtcattgctttctgcttttccacgcccgcgccc 45
gctctcgcagcgtcattgctttctgcttttccacgcccgcgccc 90
atgccctgctcgaagatgccgcgccgctctctgcctccaagagg 135
M P C S E D A A A V S A S K R 15
gctcgcagcggaggatggcgcttctctgcgcttcgctgcggtctcg 180
A R A E D G A S L R F V R L S 30
gagcacgccacggcgcccaccgcggggtccgcgcgctgcggc 225
E H A T A P T R G S A R A A G 45
tacgacctattcagtgctatgattatacaatatacaccatggag 270
Y D L F S A Y D Y T I S P M E 60
aaagccatcgtgaagacagacattcagatagctgtcccttctggg 315
K A I V K T D I Q I A V P S G 75
tgctatggaagagtagctccacgcttctggcttggtgtaaacgac 360
C Y G R V A P R S G L A V K H 90
ttcatagatgtaggagctggtgtcatagacgaggattacagagga 405
F I D V G A G V I D E D Y R G 105
aacgttggggtcgtgctgtttaactttgggaaagagaagtttgaa 450
N V G V V L F N F G K E K F E 120
gtgaaaaaaggatgatcggttcgagctcatctgtgagcggatt 495
V K K G D R I A Q L I C E R I 135
tcttatccagacttagaggaagtgcagaccctggatgacaccgag 540
S Y P D L E E V Q T L D D T E 150
agaggctcaggaggcttcggctccaccgggaagaattagaacttt 585
R G S G G F G S T G K N * 162
gctggaagtatctcgtgctttcaactggaaaccagaagctcta 630
acttcggaagcatttggtgttctaggatgcaggaaaggagacctc 675
gatcacatcacggttggaacgattctgttccctgggtgaggtcgcc 720
tgtaagtctgcactgtgagcatggcattgacatgcagacttgga 765
aaaccagggtacagtttagatTTTTTgttgttattatttta 810
aattatagccttccaaaactgTTTTTgatcataattgctgtatc 855
atttgaattTTTTTaatccaaataaagttgtcttttagcaaaaa 900
aaaaaaaaaaaaa 913

```

FIG. 1A. Nucleotide and amino acid sequences of murine dUTPase cDNA and sequence alignment. The nucleotide and predicted amino acid sequences of murine dUTPase are shown. The initiation ATG codon is shown in bold. The predicted amino acid sequence is indicated below the second nucleotide of each codon, and the termination codon TAG is shown in bold with an asterisk. The polyadenylation signal is underlined. The in-frame stop codon TAG at nucleotide position 43 upstream of the first ATG is underlined and bolded. GenBank™ accession number for murine dUTPase is AF091101.

(Amersham Pharmacia) and T4 polynucleotide kinase (Promega) at 37°C for 45 min. Labeled oligonucleotide was annealed with 2 µg mouse liver poly(A)<sup>+</sup> RNA at 42°C and was extended by using avian myeloblastosis virus reverse transcriptase (Promega). The resulting products were analyzed on 6% polyacrylamide, 7 M urea gel.

#### Generation of Luciferase Reporter Constructs, Transient Transfection, and Luciferase Assay

Different truncated DNA fragments of 5'-flanking region of mouse dUTPase gene were subcloned in pGL3-Basic vector (Promega). They are designated dUTPase-LucXD (-27 to -278 bp); dUTPase-LucXC (-27 to -1479 nucleotides); dUTPase-LucXB (-27 to -2557 nucleotides); dUTPase-LucXA (-27 to -3284 nucleotides); dUTPase-LucX (-27 to -3968 nucleotides). All constructs were confirmed to have the correct sequence by DNA sequencing. CV-1 cells (1 × 10<sup>5</sup>) were cultured in Dulbecco's modified Eagle's

medium containing 10% fetal calf serum. Cells were transfected for 5 h with 1.25 µg of luciferase reporter plasmid DNA, 0.75 µg of appropriate expression plasmid DNA, and 0.5 µg of β-galactosidase expression vector pCMVβ (Clontech) DNA using *N*-[1-(2,3-dioleoyloxy)propyl]-*N,N,N*-trimethylammonium methylsulfate-mediated transfection method (Boehringer Mannheim). Cell extracts were prepared 36 h after transfection and assayed for luciferase and β-galactosidase activities (Tropix, Bedford, MA).

## RESULTS

### Isolation and Nucleotide Sequence of Mouse dUTPase cDNA

By screening a newborn mouse kidney cDNA library with rat liver dUTPase cDNA probe (8) we obtained a consensus cDNA sequence that extended from the 3' poly(A)<sup>+</sup> end to nucleotide position +118

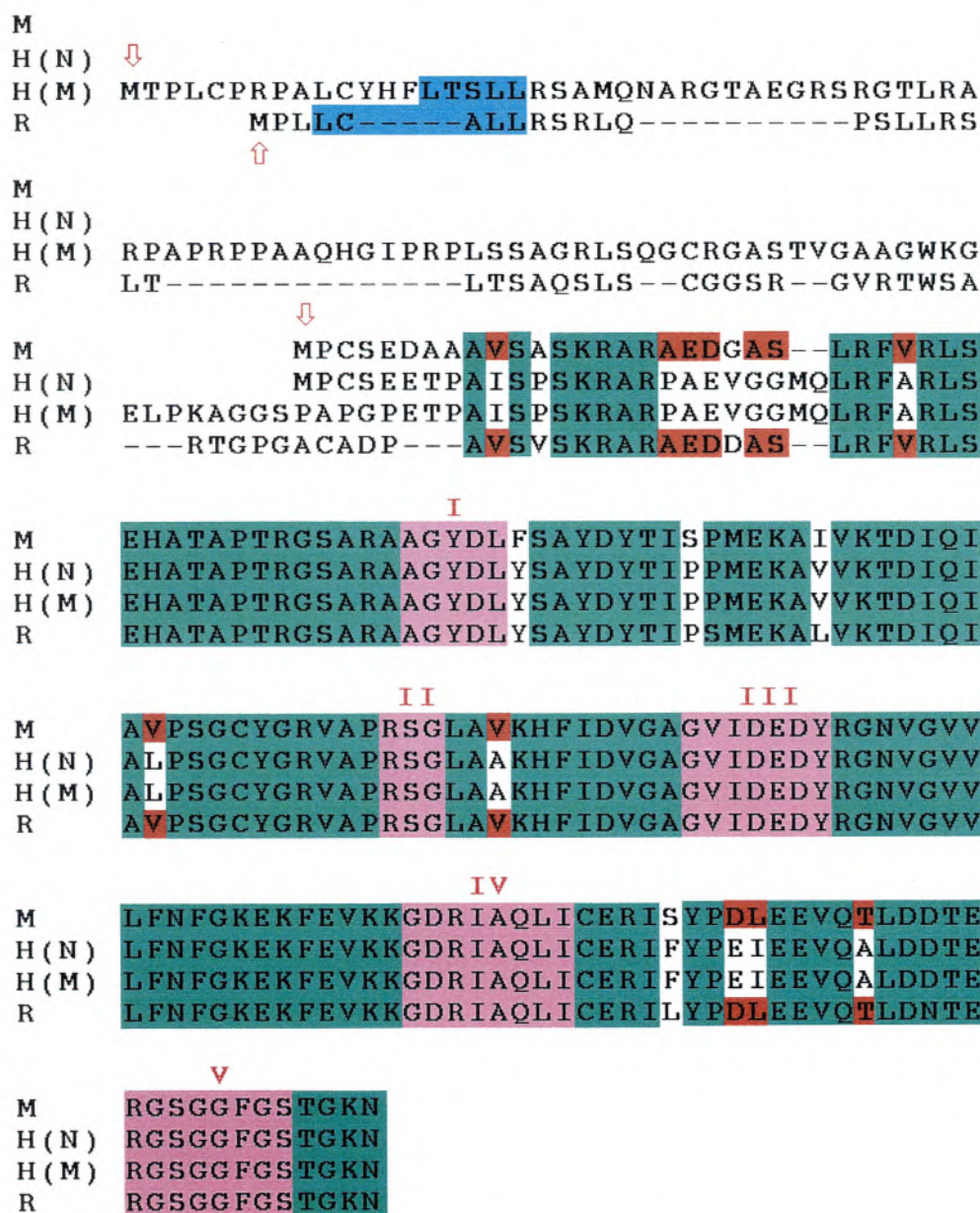


FIG. 1B. Alignment of the deduced amino acid sequences of murine (M), and rat (R) dUTPases (GenBank™ accession number U64030) with human nuclear [H(N)] dUTPase (GenBank™ accession number U31930) and human mitochondrial [H(M)] dUTPase (GenBank™ accession number U90223). The sequences (single letter codes) were aligned with Bestfit program of the GCG sequence analysis software package. Gaps were introduced to obtain optimal alignment and denoted by dashes. Identical amino acids among the four proteins are shown in green and the five evolutionarily conserved motifs (I to V) (34) in dUTPase are shown in pink. In addition, identical amino acids between only rat and murine proteins are depicted in red. The LXXLL motif known to facilitate the interaction of different proteins with nuclear receptors found in rat dUTPase and human mitochondrial dUTPase is shown in blue. The red arrows indicate the starting methionine residues for each protein.

on the mouse dUTPase sequence. The remaining 5' region was characterized by performing the rapid amplification of 5' cDNA ends, and the full-length murine dUTPase cDNA was then obtained by RT-PCR amplification using gene-specific primers. The sequence information on a putative full-length mouse liver dUTPase cDNA is depicted in Fig. 1 (GenBank™

accession number AF091101). The nucleotide sequence of 913 base pairs contains a single open reading frame of 486 913 base pairs encoding a polypeptide of 162 amino acids, and followed by a 337-bp 3'-untranslated region that contains the polyadenylation signal at nucleotide position 877 (Fig. 1A). The calculated molecular mass of the deduced amino acid

sequence is ~17.4 kDa. The start of the coding sequence was defined by the first ATG downstream of an in-frame stop codon at nucleotide position 43. The sequences (GCCGCCATGCCCTGC) surrounding ATG essentially conform to a consensus sequence for the translation initiation site (24). A homology search revealed that the coding sequence of mouse dUTPase is ~87% identical to that of human nuclear dUTPase (Fig. 1B). Human nuclear dUTPase consists of 164 amino acids (28), whereas murine dUTPase reported here has 162 amino acids (Fig. 1B). Of interest is that the rat dUTPase differs from both murine and human nuclear dUTPases in that it contains 205 amino acids, but resembles somewhat the human mitochondrial dUTPase (26). Both rat and human mitochondrial dUTPases are longer at the NH<sub>2</sub>-terminal region. The rat dUTPase has 43 extra amino acids compared to murine dUTPase. The human mitochondrial dUTPase reveals 88 extra amino acids at the NH<sub>2</sub>-terminal region when compared to human nuclear dUTPase (28). Of special interest is that the NH<sub>2</sub>-terminal extensions of both rat and human mitochondrial dUTPases contain an LXXLL signature motif. This LXXLL motif is known to facilitate the interaction of nuclear receptor cofactors with nuclear receptors (15,48). Nonetheless, the C-terminal portions of rat dUTPase and human mitochondrial dUTPase are remarkably similar in deduced amino acid sequences to murine dUTPase and human nuclear dUTPase (Fig. 1B).

#### Mouse dUTPase Does Not Bind to PPAR $\alpha$

In an earlier study, we showed that the N-terminal 62-amino acid peptide of rat dUTPase interacts with PPAR $\alpha$  (8). The mouse dUTPase we cloned in the present study is essentially identical to the rat dUTPase except that it lacks 43 amino acids at the N-terminal end (Fig. 1B). The 62-amino acid N-terminal portion of rat dUTPase that interacts with PPAR $\alpha$  has 19 amino acids that are similar to the N-terminal 19 amino acids of mouse dUTPase (Fig. 1B). We assessed the binding of full-length mouse dUTPase to PPAR $\alpha$  using the GST pulldown assay and found that mouse enzyme fails to interact with PPAR $\alpha$  (Fig. 2). As was previously noted, the full-length rat dUTPase did bind to PPAR $\alpha$  (Fig. 2). A closer look at the N-terminal rat dUTPase amino acid sequence that is not part of the mouse enzyme reveals LXXLL signature motif (Fig. 1B), and this motif is essential for the interaction of proteins with nuclear receptors (15,48). It is also of interest to note that human mitochondrial dUTPase also has a LXXLL motif in the N-terminal region (Fig. 1B) (26). Like mouse dUTPase, the human nuclear dUTPase lacks this LXXLL signature motif (28). Accordingly, the

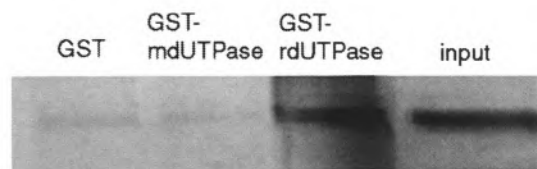


FIG. 2. In vitro interaction of dUTPase with PPAR $\alpha$ . [<sup>35</sup>S]Methionine-labeled PPAR $\alpha$ , generated by in vitro transcription and translation, was incubated with GST-Sepharose beads bound with purified *E. coli*-expressed GST-mouse dUTP (GST-mdUTPase) and GST-rat dUTPase (GST-rdUTPase). The bound proteins were eluted and analyzed by SDS-PAGE and autoradiographed. Note that PPAR $\alpha$  binds rat dUTPase but not mouse dUTPase. No binding is seen to GST alone, which served as control. In the lane marked input, 1  $\mu$ l of translated receptor protein from a standard reaction was used as control.

inability of mouse dUTPase to bind to PPAR $\alpha$  is most likely due to the absence of this LXXLL receptor binding motif.

#### Tissue Distribution and Developmental Expression

The expression of dUTPase was examined in a variety of adult mouse tissues by Northern blot analysis. A transcript size of ~1 kb has been detected with strongest expression in testis, liver, and heart and at lower levels in kidney and spleen (Fig. 3). In testis and liver two additional transcripts ranging in size from 1.9 to 2.2 kb were also detected, suggesting the possible existence of isoforms of this enzyme (Fig. 3). We then examined the expression of dUTPase mRNA in adult tissues and during mouse embryogenesis by in situ hybridization using <sup>35</sup>S-labeled anti-sense dUTPase RNA probe. In the adult mouse, significant dUTPase mRNA signal was detected in the epithelium lining the crypts of intestinal mucosa (Fig. 4A, B) and in the dividing layers of germinal epithelium, namely spermatocytes, of testis (Fig. 4D). Immunoperoxidase staining for dUTPase further confirmed the specific expression of this protein in intestinal crypts and the proliferating cells of germinal epithelium (Fig. 4C, E). In the adult mouse testis, the expression of dUTPase in cells coincided with the expression of proliferating cell nuclear antigen (PCNA) (Fig. 4F). Similar concordance between dUTPase expression (Fig. 4J, K) and PCNA expression (Fig. 4L) was also noted in embryonic testis. In the immature testis of a 2-week-old mouse we did not observe any appreciable levels of dUTPase and PCNA (Fig. 4G, H, I), suggesting a possible role for dUTPase in cell proliferation. The dUTPase signal was also found in spleen, thymus, and few cells of the basal epithelium of epidermis but the labeling intensity was substantially lower in these tissues compared to intestine and testis (data not shown). We ex-

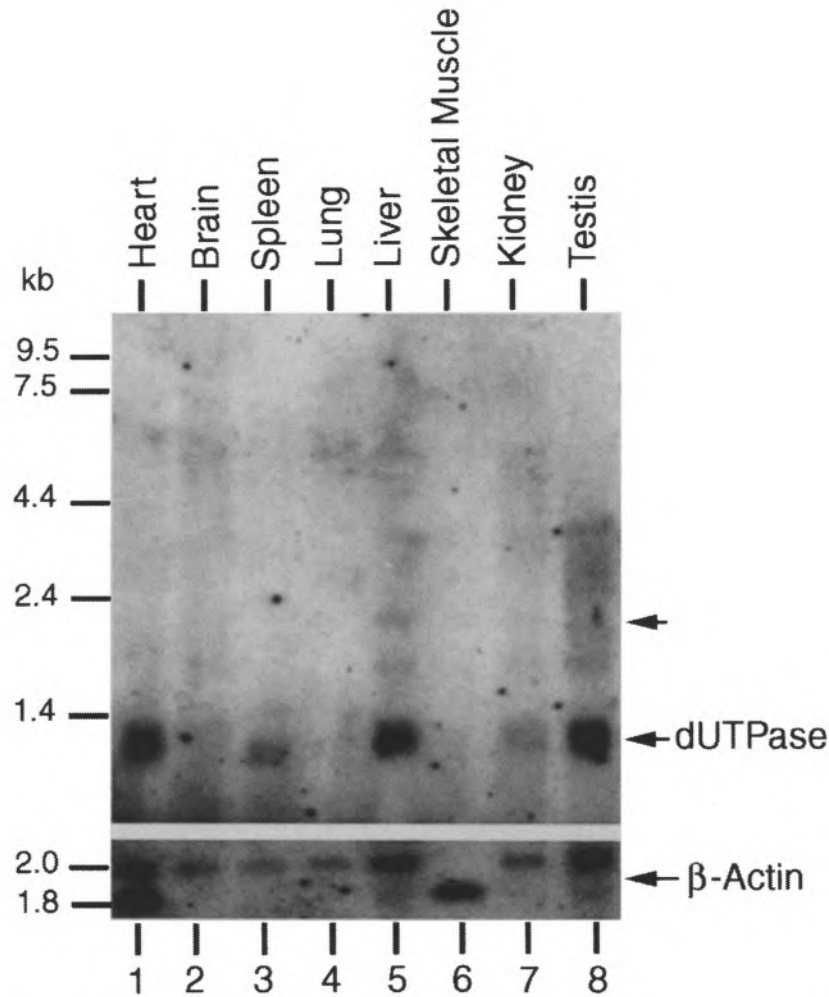


FIG. 3. Northern blot analysis of dUTPase mRNA. A mouse multiple tissue Northern blot (Clontech) containing 2  $\mu$ g of poly(A)<sup>+</sup> RNAs from each of the indicated normal adult tissue was probed with <sup>32</sup>P-labeled dUTPase cDNA. The film was exposed for 24 h. The major transcript (arrow) in testis, liver, spleen, heart, and kidney is ~900 bp. Two minor transcripts are also shown (arrow heads). The blot was reprobed with  $\beta$ -actin cDNA to assess RNA loading. One or both isoforms of  $\beta$ -actin are found in these tissues.

amined the expression of dUTPase in mouse embryos ranging in gestational age from E9.5 days to E15.5 days. The dUTPase was expressed predominantly in developing neural epithelium, and hepatic primordium in the mouse embryo at E9.5 days and its expression began to be localized to the developing liver, kidney, gut, thymus, seminiferous tubules, and lung (Figs. 5 and 6). In the developing brain dUTPase expression was prominent in the granular layer of cerebellum, ventricular zone, olfactory epithelium, and choroid plexus at E13.5 and E15.5 days (Figs. 5 and 6).

#### *Genomic Structure and Identification of the Transcription Start Site*

To isolate the dUTPase gene, a murine P1 bacteriophage library was screened, and two P1 clones

(18864 and 18865) exhibiting similar restriction fragment patterns were found. Hence we characterized only clone 18865, which contained the entire dUTPase gene. The dUTPase gene spans ~13 kb and contains 6 exons ranging in size from 45 bp (exon 3) to 391 bp (exon 6) (Table 1). The identified exon/intron junctions (Table 1) were all in agreement with the consensus 5' GT and 3' AG sequences (4). Transcription start sites were determined using primer extension analysis and 5'-RACE using poly(A)<sup>+</sup> RNA from mouse liver. We performed primer extension with a <sup>32</sup>P-end-labeled 30-mer oligonucleotide and identified a major transcription start site in a 3-base pair stretch (data not shown). This site is 90 nucleotides upstream of the translation initiating ATG codon. The PCR product from the RACE reaction consisted of a single band that, upon sequencing, also

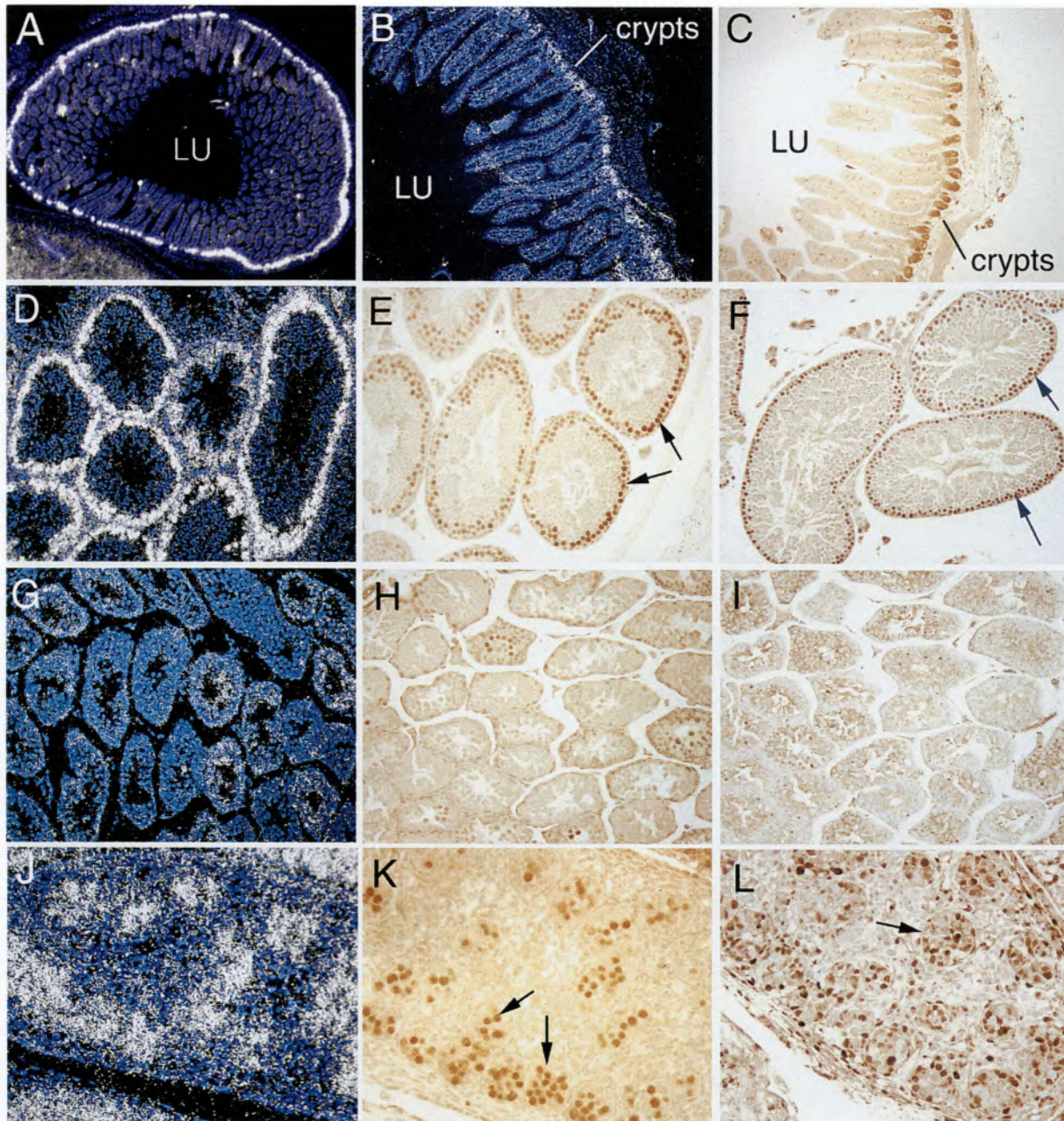


FIG. 4. Expression of dUTPase gene in the intestinal mucosa and the testis visualized by in situ hybridization and immunohistochemistry. In situ hybridization with a  $^{35}\text{S}$ -labeled antisense dUTPase RNA probe (A, B, D, G, and J) and immunohistochemical localization of dUTPase (C, E, H, and K) and PCNA (F, I, and L) of the intestine (A–C) and the testis (D–L). (A) (cross-section) and (B) (longitudinal section) adult mouse intestine depicting intense labeling in the crypts by in situ hybridization and (C) shows similar staining pattern for dUTPase by immunohistochemical reaction. (D) In situ hybridization for dUTPase in adult testis, and (E) and (F) parallel sections stained immunohistochemically for dUTPase and PCNA, respectively, reveal that dUTPase expression is confined to the proliferating cell compartment of the germinal epithelium. (G, H, I) Sections of immature quiescent testis of 2-week-old mouse showing no detectable expression of dUTPase (G, H) and PCNA (I). (J, K, L) Sections of developing testis of E15.5 day embryonic mouse exhibiting similar patterns of expression for dUTPase (J, K) and PCNA (L). LU, lumen. Arrows point to cells positively stained.



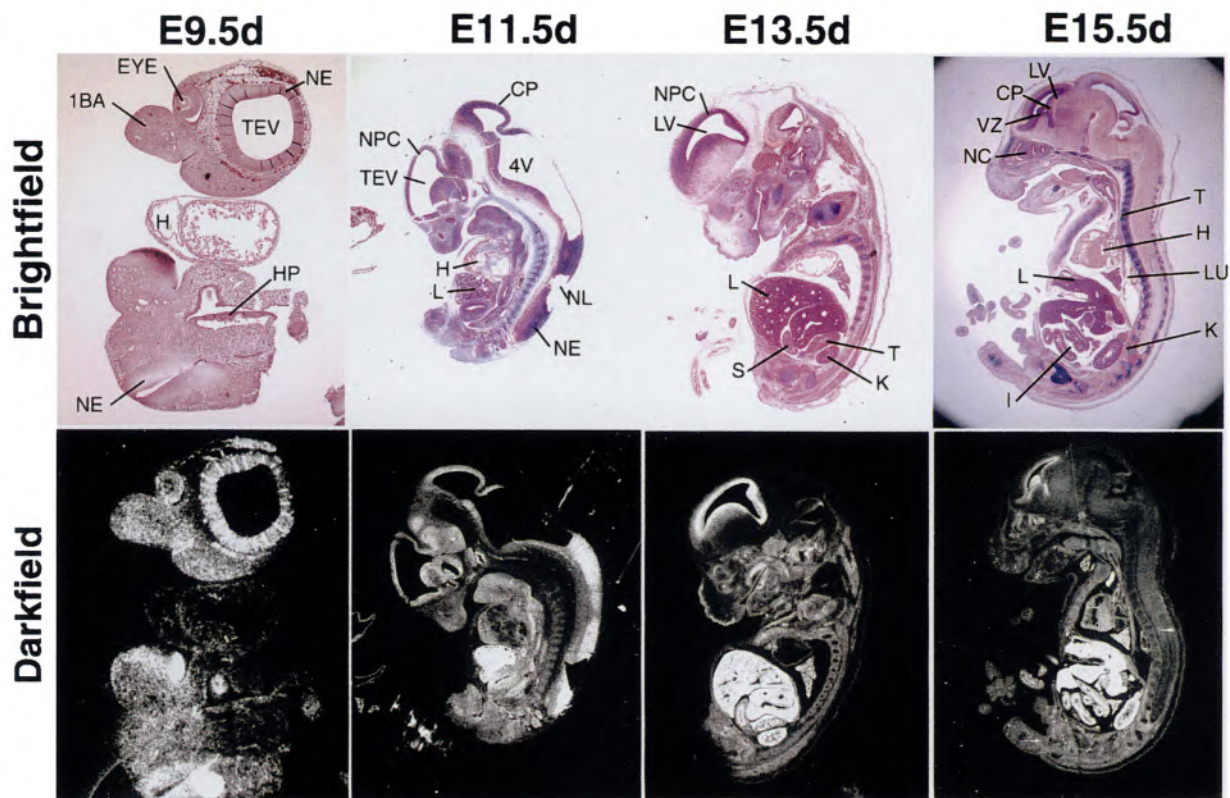


FIG. 5. In situ hybridization (ISH) analysis of murine dUTPase mRNA expression in mouse embryos. Bright-field and dark-field sagittal sections of 9.5 (E9.5d), 11.5 (E11.5d), 13.5 (E13.5d), and 15.5 (E15.5d) day mouse embryos. Dark-field illustrations show strong expression of dUTPase in the neural epithelium (NE), hepatic primordium (HP), first brachial arch (1BA), and eye in 9.5-day embryo; neopallial cortex (NPC), cerebellar primordium (CP), neural epithelium (NE), and liver (L) in 11.5-day embryo; neopallial cortex (NPC), liver (L), stomach (S), kidney (K), and testis (T) in 13.5-day embryo; and in liver (L), thymus (TH), lung (Lu), testis (T), kidney (K), intestines (I), choroid plexus (CH), and nasal cavity (NC) in 15.5-day embryo. TEV, telencephalic vesicle; H, heart; 4V, fourth ventricle; NL, neural lumen; LV, lateral ventricle; VZ, ventricular zone.

revealed a sequence terminating at the nucleotide T, 90 nucleotides upstream of the translation initiation codon ATG. This nucleotide position has been designated +1 (Fig. 7).

#### *Potential Transcription Factor Binding Sites in the 5' Upstream Region and Functional Analysis of the Mouse dUTPase Promoter*

Genomic sequences 3968 bp upstream of the transcription start site were cloned and sequenced (partial sequence information shown in Fig. 7). The 5'-flanking region contained TATA box in proximity to the putative transcription start site (position -43 to -40). A 392-bp region upstream from the TATA box is highly rich (77%) in C and G nucleotides and contains a number of putative response elements. These include sequence matches for AP4, Sp1, AP2, Ker1, MAZ, CREB, CACC-binding factor, and RREB, among others (Fig. 7). To determine the importance of regulatory regions for the expression of the dUTPase gene, the region between nucleotides -3968 and -27 as well as four deletion constructs of this

promoter were subcloned into the pGL3-Basic Luciferase vector. All constructs had variable 5' ends to the same *Xho*I cleavage at -27 relative to the transcription start site. Promoter activity was analyzed after transient transfection into CV-1 cells and results are summarized in Fig. 8. The luciferase activity was increased by deletion from nucleotides -3968 to -278. The plasmids dUTPase-LucXC (nucleotides -1479 to -27) and dUTPase-LucXD (nucleotides -278 to -27) showed maximal promoter activity (Fig. 8). The plasmid dUTPase-LucXBB, with deletion of nucleotides -1479 to -278 from plasmid dUTPase-LucXB (-2557 to -27) substantially reduced the promoter activity, suggesting that nucleotides -1479 through -278 possibly contain enhancer sequences and the sequences upstream of -1479 may exert repressor effect.

#### DISCUSSION

In a previous study, using the yeast two-hybrid system to identify proteins that interact with PPAR $\alpha$ ,

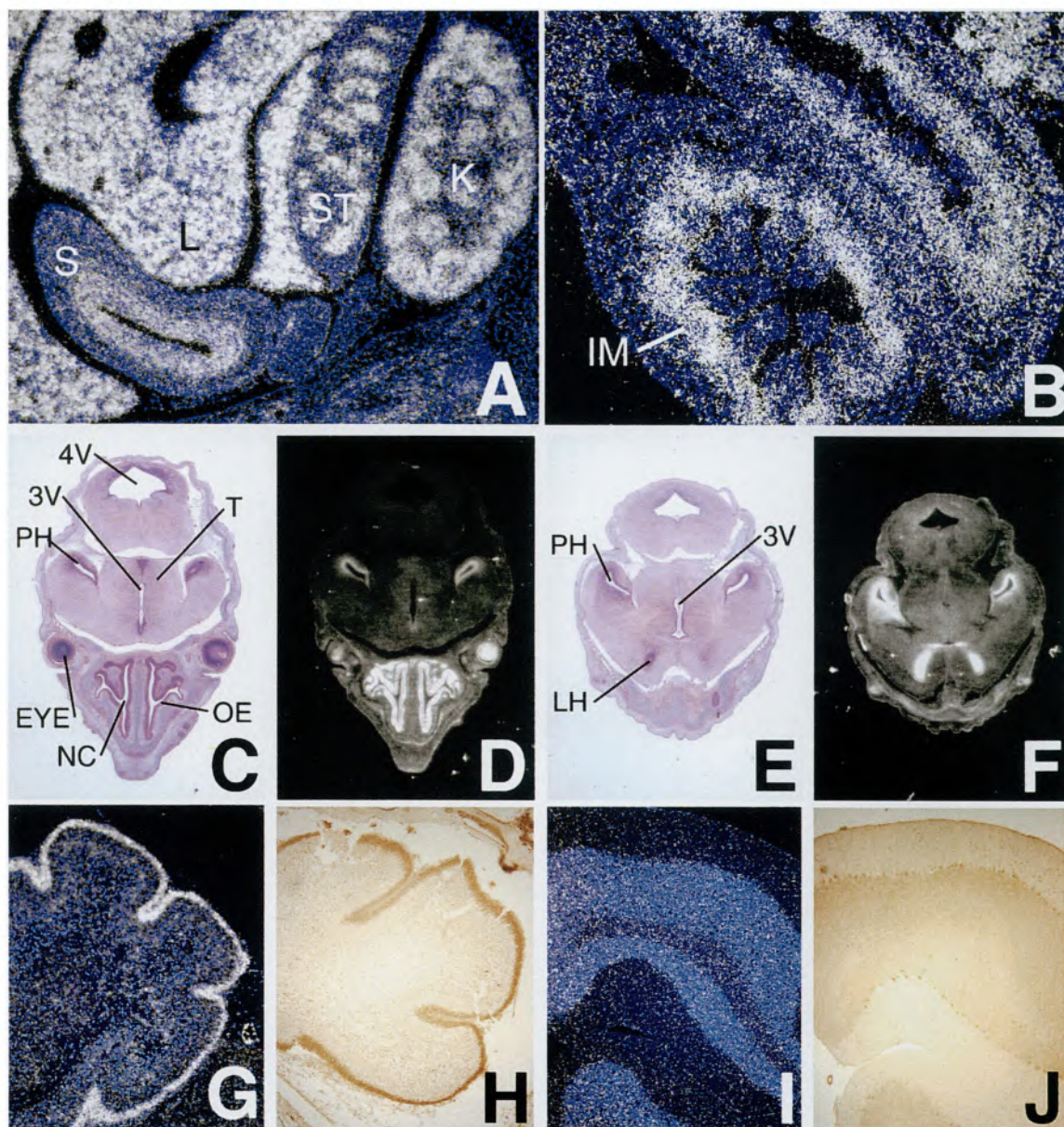


FIG. 6. Expression of dUTPase in selected embryonic mouse tissues. In situ hybridization with a  $^{35}\text{S}$ -labeled antisense dUTPase RNA probe (A, B, D, F, G) and immunohistochemical localization of dUTPase (H, J). (C, E) Bright-field illustrations corresponding to (D) and (F), respectively. (A) High magnification of E13.5-day mouse embryo showing intense labeling of liver (L), developing seminiferous tubules (ST) of testis, neogenic glomeruli in kidney (K), mucosa of stomach (S). (B) High magnification of intestinal mucosa (IM) of E15.5-day mouse embryo. (C–F) Sections of brain of an E15.5-day mouse embryo at different levels. Intense labeling is observed in olfactory epithelium (OE), lining of the nasal cavity (NC), the posterior (PH), and lateral horn (LH) of third ventricle. The positions of thalamus (T), third ventricle (3V), and fourth ventricle (4V) and eye are indicated. (G, H) Sections of cerebellum of an E15.5-day embryo showing expression of dUTPase mRNA (G) and protein (H) in the granular layer. (I, J) Sections of adult mouse cerebellum showing no appreciable expression of dUTPase mRNA (I) and protein (J).

we isolated and characterized rat dUTPase as a PPAR-interacting protein (8). Rat dUTPase prevented the formation *in vitro* of PPAR-RXR heterodimers and inhibited the transcriptional activity of all three isoforms of PPAR ( $\alpha$ ,  $\delta$ , and  $\gamma$ ). We also showed that when PPAR $\alpha$  and dUTPase were transiently coexpressed in human embryonic kidney

cells, these proteins appeared to colocalize within the nucleus (8). The interaction of PPAR $\alpha$  was shown to be with the N-terminal 62-amino acid region of rat dUTPase (8). These observations suggested the necessity of cloning dUTPase cDNAs from other species, such as the mouse, that are responsive to peroxisome proliferators, so as to enhance our understand-

TABLE 1  
ORGANIZATION OF MOUSE dUTPase GENE

Exon Size (bp)	Intron			Exon
	Splice Donor	Size (bp)	Splice Acceptor	
1 (239)	ATTCAG <b>gt</b> gagg	(1254)	ttcagTGCCTA	2
2 (92)	GAGTAG <b>gt</b> aagt	(1707)	ctttagCTCCAC	3
3 (45)	TAGGAG <b>gt</b> aaca	(5822)	ctccagCTGGTG	4
4 (75)	TTGAAG <b>gt</b> gagt	(147)	ttgaagTGAAAA	5
5 (71)	GTGCAG <b>gt</b> gagt	(216)	ttcagACCCTG	6
6 (391)*				

The exonic sequences are shown in capital letters. The splice donors GT and the splice acceptors AG are shown in bold letters.

\*Length includes the sequenced portion of 3'-noncoding region.

ing of the functional significance of dUTPase binding to PPAR $\alpha$ .

In the present study, we show that murine dUTPase cDNA contains a 162-amino acid open reading frame encoding a protein with a predicted  $M_r$  of 17,400. The murine enzyme differs from the rat dUTPase in that it is 43 amino acids shorter at the N-terminal end and fails to interact with PPAR $\alpha$ . The extra 43-amino acid N-terminal extension of rat dUTPase contains one LXXLL motif (at 4–8 amino acids); one or more of these LXXLL signature sequence motifs have recently been shown to be necessary and sufficient for the interaction of transcriptional coactivators with the nuclear receptors (15,48). There is also a second LXXLL motif, albeit in reverse orientation (LLXXL at 16–20 amino acids) in rat dUTPase. The presence of a LXXLL motif in the N-terminal 62-amino acid region of rat dUTPase and its absence in murine dUTPase might account for the differential binding of these two proteins to PPAR $\alpha$ . The human nuclear dUTPase cDNA, with a 164-amino acid open reading frame, is similar to the 162-amino acid-containing murine dUTPase and also lacks LXXLL motif (28), raising the possibility that human dUTPase might not interact with PPAR $\alpha$ .

The recently cloned mitochondrial form of human dUTPase (with 252 amino acids) is even longer than the rat dUTPase (with 205 amino acids) and contains one LXXLL motif (at 15–19 amino acids) in the N-terminal extension (26). In the human mitochondrial dUTPase, the LXXLL motif is in the arginine-rich N-terminal mitochondrial targeting presequence (26). In rat dUTPase, this motif is also in the arginine-rich N-terminal extension, raising the possibility that this arginine-rich segment could serve as mitochondrial targeting signal peptide. However, preliminary observations suggest that this enzyme is not mitochondrial because in vitro expressed rat dUTPase was not cleaved when incubated with mitochondria. Further-

more, in cells transiently expressing dUTPase, the protein was observed predominantly in the cytosol with a weak signal in the nucleus; when dUTPase and PPAR were coexpressed both proteins were found colocalized within the nucleus (8). These observations suggest that multiple forms of dUTPase exist in mammals and isoforms containing LXXLL motif interact with nuclear receptors. Northern blots of mouse tissues show the presence of one or more minor transcripts, which may represent the isoforms with LXXLL motif similar to the one of rat dUTPase. Likewise, the possibility exists that rat tissues may contain a dUTPase similar to the mouse dUTPase reported in this study. Because the human dUTPase gene encodes both nuclear and mitochondrial isoforms, the possibility exists that the mouse and rat genes may encode different isoforms (26). Further studies, in particular site-directed mutagenesis involving the LXXLL motif, are needed to assess the role of LXXLL motif in rat dUTPase in protein-protein interaction.

Although one or more LXXLL sequence motifs are commonly discerned in nuclear receptor coactivators [such as SRC-1 (25,53), PBP (54), ACTR/AIB1 (1,7), and others (13)], these are also found in other receptor cofactors (e.g., RIP140), which downregulate nuclear receptor activity by competition with coactivators for receptor binding (49). Of the many coactivators identified so far (13), SRC-1 (53), PBP (54), CBP/p300 (11), and PGC-1 (43) have been found to serve as coactivators for PPARs. In this regard, rat dUTPase may function as a repressor by binding to PPAR (8). Although the N-terminal 62-amino acid portion of dUTPase has been shown to bind to PPAR, studies are needed to determine if dUTPase interacts with the extreme C-terminus of the receptor, on the AF-2 domain, which has been shown to be the docking site for many coactivators (13,53,54). Immunohistochemical studies using poly-



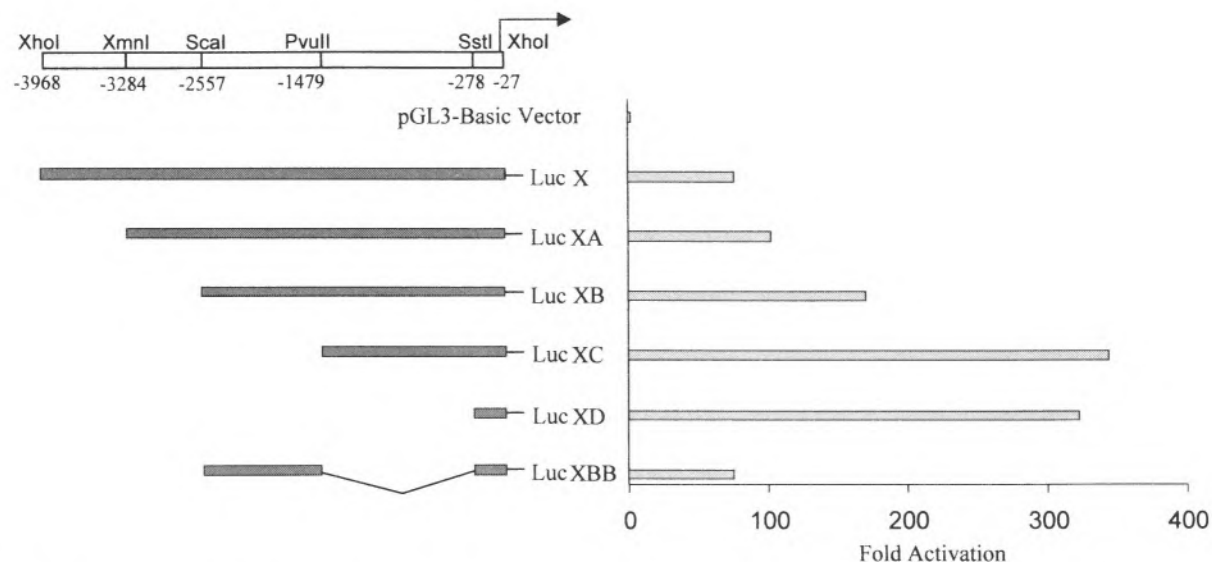


FIG. 8. The murine dUTPase promoter activity. The schematic diagram on the left represents each construct of the dUTPase gene (dark box) fused into the upstream region of the luciferase gene (Luc) with variable 5' ends to the -27 nucleotide relative to the transcription start site. The -3968 to -27 segment (dUTPase-LucX) was cloned into *XhoI* site, and the other constructs, after digesting with restriction enzymes shown, were cloned into pGL3-Basic. The constructs have been designated dUTPase-LucX, XA, XB, XC, XD, and XBB. Each construct was transiently transfected into CV-1 cells. The promoter activity is expressed as fold induction relative to the promoterless pGL3-Basic vector. The data are the mean of triplicate determinations. Deletion of a region, -1479 to -278, from dUTPase-LucXB results in substantial reduction in promoter activity.

first time the visual evidence of the presence of this enzyme only in cells that are synthesizing DNA.

The interaction of rat dUTPase with PPARs suggests that dUTPase could possibly serve as a repressor of differentiation by inhibiting the activity of these transcription factors. Analysis of dUTPase expression by in situ hybridization using mouse dUTPase cDNA probe clearly showed that cells actively synthesizing DNA, such as those in the crypts of intestinal mucosa and in the germinal epithelium of testis, have the highest levels of dUTPase mRNA in the adult mouse (Fig. 4). In the adult mouse intestinal mucosa, both in situ hybridization and immunoperoxidase methods revealed the expression of dUTPase only in cells comprising the crypts but not in differentiated cells along the villous. Similar expression pattern was detected in rat intestinal mucosa (unpublished observations). In contrast to the cell proliferation-dependent expression of mouse and rat dUTPase, high levels of PPAR $\gamma$  expression are detected throughout the mucosal villous (20), suggesting that dUTPase expressed in cells of the crypts possibly represses PPAR function, and once dUTPase expression is turned off following DNA synthesis and cell division, the PPARs may then influence differentiation as the cells migrate apically along the villous and differentiate. During embryonic development dUTPase expression occurs in actively proliferating tissues of brain, liver, intestinal mucosa, and thymus,

among others. The expression of dUTPase during embryogenesis appears to correlate with the expression of PCNA in the same cells, further confirming that dUTPase belongs to a class of S-phase-specific genes that are expressed in a growth-dependent manner (16,17, 26,40). In fetal testis, we found a high level of expression of dUTPase in rapidly developing germinal epithelium, but the level of expression was undetectable in the testis of immature preweaning mouse. As indicated above, the expression of dUTPase gene was robust in a single layer of proliferating seminiferous epithelial cells in the adult testis. The expression of dUTPase coincides with the onset of DNA replication. There is evidence to suggest that human nuclear form of dUTPase is serine phosphorylated at a cyclin-dependent protein kinase phosphorylation site (27), but the human mitochondrial form of dUTPase, although containing a consensus site, does not undergo phosphorylation (26). Sequence comparison of human nuclear dUTPase, human mitochondrial dUTPase, rat dUTPase, and murine dUTPases reveals five conserved domains (Fig. 1B) and the murine dUTPase also reveals Ser-11 in context to the consensus target sequence of cyclin-dependent kinase, p34<sup>cdc2</sup> (22). Whether this Ser-11 site could be phosphorylated in murine dUTPase similar to that noted for human nuclear form of dUTPase remains to be ascertained.

Finally, our current knowledge of the mechanism

governing the expression of dUTPase is limited. Recently, the dUTPase gene was isolated from *Candida albicans* (36) and humans (26). The human dUTPase gene encodes both nuclear and mitochondrial isoforms of dUTPase through the use of alternative 5' exons (26), and the 5'-flanking region directly upstream of nuclear form of dUTPase contains putative binding sites for certain transcription factors responsible for transcriptional activation of S-phase induction (26,39). As illustrated in Figs. 7 and 8, the 5'-flanking region directly upstream of murine dUTPase, which exhibited high promoter activity, contains several putative sites for transcription factor binding such as Sp1 (39), MAZ (19), Ker1 (30), RVF (50), CREB (44), RREB (46), and CACCC-binding factor (51). Some of these factors, such as RVF, are known to enhance the transcriptional activity while

others, such as MAZ, function as transcriptional repressors. Differential binding of these transcription factors at different phases of cell cycle can influence dUTPase gene expression. Further work is required to determine which transcription factors play a central role in the dUTPase gene transcription and the relationship between dUTPase expression and possible repression of differentiation.

#### ACKNOWLEDGMENTS

This work was supported by National Institutes of Health Grants GM 23750 (to J.K.R.) and DK28492 (Y.S.K), and Veterans Affairs Merit Review grants (to A.V.Y. and M.S.R.), and the Joseph L. Mayberry Sr. Endowment Fund.

#### REFERENCES

1. Anzick, S. L.; Kononen, J.; Walker, R. L.; Azorsa, D. O.; Tanner, M. M.; Guan, X. Y.; Sauter, G.; Kallioniemi, O. P.; Trent, J. M.; Meltzer, P. S. AIB1, a steroid receptor coactivator amplified in breast and ovarian cancer. *Science* 277:965-968; 1997.
2. Barclay, B. J.; Kunz, B. A.; Little, J. G.; Haynes, R. H. Genetic and biochemical consequences of thymidylate stress. *Can. J. Biochem.* 60:172-194; 1982.
3. Bravo, R.; Fey, S. J.; Bellatin, J.; Mose-Larsen, P.; Arvalo, J.; Celis, J. E. Identification of a nuclear and of a cytoplasmic polypeptide whose relative proportions are sensitive to changes in the rate of cell proliferation. *Exp. Cell Res.* 136:311-319; 1981.
4. Breathnach, R.; Benoist, C.; O'Hare, K.; Gannon, F.; Chambon, P. Ovalbumin gene: Evidence for leader sequence in mRNA and DNA sequences at the exon-intron boundaries. *Proc. Natl. Acad. Sci. USA* 75:4853-4857; 1978.
5. Canman, C. E.; Radany, E. H.; Parsels, L. A.; Davis, M. A.; Lawrence, T. S.; Maybaum, J. Induction of resistance to fluorodeoxyuridine cytotoxicity and DNA damage in human tumor cells by expression of *Escherichia coli* deoxyuridine triphosphatase. *Cancer Res.* 54:2296-2298; 1994.
6. Cedergren-Zeppezauer, E. S.; Larsson, G.; Nyman, P. O.; Dauter, Z.; Wilson, K. S. Crystal structure of a dUTPase. *Nature* 355:740-743; 1992.
7. Chen, H.; Lin, R. J.; Schiltz, R. L.; Chakravarti, D.; Nash, A.; Nagy, L.; Privalsky, M. L.; Nakatani, Y.; Evans, R. M. Nuclear receptor coactivator ACTR is a novel histone acetyltransferase and forms a multimeric activation complex with P/CAF and CBP/p300. *Cell* 90:569-580; 1997.
8. Chu, R.; Lin, Y.; Rao, M. S.; Reddy, J. K. Cloning and identification of rat deoxyuridine triphosphatase as an inhibitor of peroxisome proliferator-activated receptor  $\alpha$ . *J. Biol. Chem.* 271:27670-27676; 1996.
9. Curtin, N. J.; Harris, A. L.; Aherne, G. W. Mechanism of cell death following thymidylate synthase inhibition: 2'-deoxyuridine-5'-triphosphate accumulation, DNA damage and growth inhibition following exposure to CB3717 and dipyridamole. *Cancer Res.* 51:2346-2352; 1991.
10. Dauter, Z.; Persson, R.; Rosengren, A. M.; Nyman, P. O.; Wilson, K. S.; Cedergren-Zeppezauer, E. S. Crystal structure of dUTPase from equine infectious anaemia virus; active site metal binding in a substrate analogue complex. *J. Mol. Biol.* 285:655-673; 1999.
11. Dowell, P.; Ishmael, J. E.; Avram, D.; Peterson, V. J.; Nevriy, D. J.; Leid, M. p300 functions as a coactivator for the peroxisome proliferator-activated receptor alpha. *J. Biol. Chem.* 272:33435-33443; 1997.
12. Gadsden, M. H.; McIntosh, E. M.; Game, J. C.; Wilson, P. J.; Haynes, R. H. dUTP pyrophosphatase is an essential enzyme of *Saccharomyces cerevisiae*. *EMBO J.* 12:4425-4431; 1993.
13. Glass, C. K.; Rose, D. W.; Rosenfeld, M. G. Nuclear receptor coactivators. *Curr. Opin. Cell Biol.* 9:222-232; 1997.
14. Gonzalez, F. J.; Peters, J. M.; Cattley, R. C. Mechanism of action of the nongenotoxic peroxisome proliferators: Role of the peroxisome proliferator-activator receptor alpha. *J. Natl. Cancer Inst.* 90:1702-1709; 1998.
15. Heery, D. M.; Kalkhoven, E.; Hoare, S.; Parker, M. G. A signature motif in transcriptional co-activators mediates binding to nuclear receptors. *Nature* 387:733-736; 1997.
16. Hokari, S.; Hasegawa, M.; Tanaka, M.; Sakagishi, Y.; Kikuchi, G. Deoxyuridine triphosphate nucleotidohydrolase: Distribution of the enzyme in various rat tissues. *J. Biochem.* 104:211-214; 1988.
17. Hokari, S.; Koyama, I.; Shioda, K.; Sakagishi, Y. Deoxyuridine triphosphatase in human hepatoma. *Int. J. Biochem.* 26:487-490; 1994.

18. Issemann, I.; Green, S. Activation of a member of the steroid hormone receptor superfamily by peroxisome proliferators. *Nature* 347:645–650; 1990.
19. Izzo, M. W.; Strachan, G. D.; Stubbs, M. C.; Hall, D. J. Transcriptional repression from the c-myc P2 promoter by the zinc finger protein ZF87/MAZ. *J. Biol. Chem.* 274:19498–19506; 1999.
20. Jain, S.; Pulikuri, S.; Zhu, Y.; Qi, C.; Kanwar, Y. S.; Yeldandi, A. V.; Rao, M. S.; Reddy, J. K. Differential expression of the peroxisome proliferator-activated receptor  $\gamma$  (PPAR $\gamma$ ) and its coactivators steroid receptor coactivator-1 and PPAR-binding protein PBP in the brown fat, urinary bladder, colon, and breast of the mouse. *Am. J. Pathol.* 153:349–354; 1998.
21. Kanwar, Y. S.; Liu, Z. Z.; Kumar, A.; Wada, J.; Carone, F. A. Cloning of mouse c-ros renal cDNA, its role in development and relationship to extracellular matrix glycoproteins. *Kidney Int.* 48:1646–1659; 1995.
22. Kennelly, P. J.; Krebs, E. G. Consensus sequences as substrate specificity determinants for protein kinases and protein phosphatases. *J. Biol. Chem.* 266:15555–15558; 1991.
23. Kliewer, S. A.; Umesono, K.; Noonan, D. J.; Heyman, R. A.; Evans, R. M. Convergence of 9-cis retinoic acid and peroxisome proliferator signalling pathways through heterodimer formation of their receptors. *Nature* 358:771–774; 1992.
24. Kozak, M. The scanning model for translation: An update. *J. Cell Biol.* 108:229–241; 1989.
25. Krey, G.; Braissant, O.; L'Horset, F.; Kalkhoven, E.; Perroud, M.; Parker, M. G.; Wahli, W. Fatty acids, eicosanoids, and hypolipidemic agents identified as ligands of peroxisome proliferator-activated receptors by coactivator-dependent receptor ligand assay. *Endocrinology* 11:779–791; 1997.
26. Ladner, R. D.; Caradonna, S. J. The human dUTPase gene encodes both nuclear and mitochondrial isoforms. Differential expression of the isoforms and characterization of a cDNA encoding the mitochondrial species. *J. Biol. Chem.* 272:19072–19080; 1997.
27. Ladner, R. D.; Carr, S. A.; Huddleston, M. J.; McNulty, D. E.; Caradonna, S. J. Identification of a consensus cyclin-dependent kinase phosphorylation site unique to the nuclear form of human deoxyuridine triphosphate nucleotidohydrolase. *J. Biol. Chem.* 271:7752–7757; 1996.
28. Ladner, R. D.; McNulty, D. E.; Carr, S. A.; Roberts, G. D.; Caradonna, S. J. Characterization of distinct nuclear and mitochondrial forms of human deoxyuridine triphosphate nucleotidohydrolase. *J. Biol. Chem.* 271:7745–7751; 1996.
29. Lee, S. S.-T.; Pineau, T.; Drago, J.; Lee, E. J.; Owens, J. W.; Kroetz, D. L.; Fernandez-Salguero, P. M.; Westphal, H.; Gonzalez, F. J. Targeted disruption of the alpha isoform of the peroxisome proliferator-activated receptor gene I mice results in abolishment of the pleiotropic effects of peroxisome proliferators. *Mol. Cell. Biol.* 15:3012–3022; 1995.
30. Lin, C. S.; Chen, Y.; Huynh, T.; Kramer, R. Identification of the human alpha6 integrin gene promoter. *DNA Cell Biol.* 16:929–937; 1997.
31. Lindahl, T. DNA repair enzymes. *Annu. Rev. Biochem.* 51:61–87; 1982.
32. Lundberg, L. G.; Thoresson, H.; Karlstrom, O. H.; Nyman, P. O. Nucleotide sequence of the structural gene for dUTPase of *Escherichia coli*. *EMBO J.* 2:967–971; 1983.
33. Mangelsdorf, D. J.; Thummel, C.; Beato, M.; Herrlich, P.; Schutz, G.; Umesono, K.; Blumberg, B.; Kastner, P.; Mark, M.; Chambon, P.; Evans, R. M. The nuclear receptor superfamily: The second decade. *Cell* 83:835–839; 1995.
34. McGeoch, D. J. Protein sequence comparisons show that the 'pseudoproteases' encoded by poxviruses and certain retroviruses belong to the deoxyuridine triphosphatase family. *Nucleic Acids Res* 18:4105–4110; 1990.
35. McIntosh, E. M.; Ager, D. D.; Gadsden, M. H.; Haynes, R. H. Human dUTP pyrophosphatase: cDNA sequence and potential biological importance of the enzyme. *Proc. Natl. Acad. Sci USA* 89:8020–8024; 1992.
36. McIntosh, E. M.; Looser, J.; Haynes, R. H.; Pearlman, R. E. MluI site-dependent transcriptional regulation of the *Candida albicans* dUTPase gene. *Curr. Genet.* 26:415–421; 1994.
37. Mercer, M. A.; Fraser, K. M.; Stockwell, P. A.; Robinson, A. J. A homologue of retroviral pseudoproteases in the parapoxvirus, orf virus. *Virology* 172:665–668; 1989.
38. Mol, C. D.; Harris, J. M.; McIntosh, E. M.; Tainor, J. A. Human dUTP pyrophosphatase: Uracil recognition by a beta hairpin and active sites formed by three separate subunits. *Structure* 4:1077–1092; 1996.
39. Nevins, J. R. E2F: A link between the Rb tumor suppressor protein and viral oncoproteins. *Science* 258:424–429; 1992.
40. Pardo, E. G.; Gutierrez, C. Cell cycle- and differentiation stage-dependent variation of dUTPase activity in higher plant cells. *Exp. Cell Res.* 186:90–98; 1990.
41. Prasad, G. S.; Stura, E. A.; McRee, D. E.; Laco, G. S.; Hasselkus-Light, C.; Elder, J. H.; Stout, C. D. Crystal structure of dUTP pyrophosphatase from feline immunodeficiency virus. *Protein Sci.* 5:2429–2437; 1996.
42. Pri-Hadash, A.; Harveven, D.; Lifschitz, E. A meristem-related gene from tomato encodes a dUTPase: Analysis of expression in vegetative and floral meristems. *Plant Cell* 4:149–159; 1992.
43. Puigserver, P.; Wu, Z.; Park, C. W.; Graves, R.; Wright, M.; Spiegelman, B. M. A cold-inducible coactivator of nuclear receptors linked to adaptive thermogenesis. *Cell* 92:829–839; 1998.
44. Somers, J. P.; DeLoia, J. A.; Zeleznik, A. J. Adenovirus-directed expression of a non-phosphorylatable mutant of CREB (cAMP response element-binding protein) adversely affects the survival, but not the differentiation of rat granulosa cells. *Mol. Endocrinol.* 13:1364–1372; 1999.
45. Strahler, J. R.; Zhu, X.-X.; Hora, N.; Wang, Y. K.; An-

- draws, P. C.; Roseman, N. A.; Neel, J. V.; Turka, L.; Hanash, S. M. Maturation stage and proliferation-dependent expression of dUTPase in human T cells. *Proc. Natl. Acad. Sci. USA* 90:4991-4995; 1993.
46. Thiagalingam, A.; De Bustros, A.; Borges, M.; Jasti, R.; Compton, D.; Diamond, L.; Mabry, M.; Ball, D. W.; Baylin, S. B.; Nelkin, B. D. RREB-1, a novel zinc finger protein, is involved in the differentiation response to Ras in human medullary thyroid carcinomas. *Mol. Cell Biol.* 16:5335-5345; 1996.
  47. Tontonoz, P.; Hu, E.; Graves, R. A.; Budavari, A. I.; Spiegelman, B. M. mPPAR gamma 2: Tissue-specific regulator of an adipocyte enhancer. *Genes Dev.* 8: 1224-1234; 1994.
  48. Torchia, J.; Rose, D. W.; Inostroza, J.; Kamei, Y.; Westin, S.; Glass, C. K.; Rosenfeld, M. G. The transcriptional co-activator p/CIP binds CBP and mediates nuclear-receptor function. *Nature* 387:677-684; 1997.
  49. Treuter, E.; Albrechtsen, T.; Johansson, L.; Leers, J.; Gustafsson, J.-A. A regulatory role for RIP140 in nuclear receptor activation. *Mol. Endocrinol.* 12:864-881; 1998.
  50. Yan, D. H.; Hung, M. C. Differential activity of the RVF enhancer element in the decreased expression of the neu oncogene in NR-6 cells versus parental Swiss Webster 3T3 cells. *Mol. Carcinog.* 7:44-49; 1993.
  51. Youssoufian, H. Further characterization of cis-acting regulatory sequences in the genomic locus of the murine erythropoietin receptor: Evidence for stage-specific regulation. *Blood* 83:1428-1435; 1994.
  52. Zhu, Y.; Alvares, K.; Huang, Q.; Rao, M. S.; Reddy, J. K. Cloning of a new member of the peroxisome proliferator-activated receptor gene family from mouse liver. *J. Biol. Chem.* 268:26817-26820; 1993.
  53. Zhu, Y.; Qi, C.; Calandra, C.; Rao, M. S.; Reddy, J. K. Cloning and identification of mouse steroid receptor coactivator-1 (mSRC-1), as a coactivator of peroxisome proliferator-activated receptor  $\gamma$ . *Gene Expr.* 6: 185-195; 1996.
  54. Zhu, Y.; Qi, C.; Jain, S.; Rao, M. S.; Reddy, J. K. Isolation and characterization of PBP, a protein that interacts with peroxisome proliferator-activated receptor. *J. Biol. Chem.* 272:25500-25506; 1997.